CI

e-med
www.e-med.org.uk

ARTICLE

Diffusion-weighted magnetic resonance imaging and its application to cancer

Elizabeth M Charles-Edwards and Nandita M deSouza

Cancer Research UK Clinical Magnetic Resonance Research Group, Institute of Cancer Research and Royal Marsden NHS Foundation Trust, Sutton, Surrey, UK

Corresponding address: Elizabeth Charles-Edwards, Cancer Research UK Clinical Magnetic Resonance Research Group, Institute of Cancer Research and Royal Marsden NHS Foundation Trust, Downs Road, Sutton, Surrey SM2 5PT, UK. E-mail: `Liz.Charles-Edwards@icr.ac.uk`

Abstract

Diffusion-weighted magnetic resonance imaging (DW-MRI) provides image contrast through measurement of the diffusion properties of water within tissues. Application of diffusion sensitising gradients to the MR pulse sequence allows water molecular displacement over distances of 1–20 μm to be recognised. Diffusion can be predominantly unidirectional (anisotropic) or not (isotropic). Combining images obtained with different amounts of diffusion weighting provides an apparent diffusion coefficient (ADC) map. In cancer imaging DW-MRI has been used to distinguish brain tumours from peritumoural oedema. It is also increasingly exploited to differentiate benign and malignant lesions in liver, breast and prostate where increased cellularity of malignant lesions restricts water motion in a reduced extracellular space. It is proving valuable in monitoring treatment where changes due to cell swelling and apoptosis are measurable as changes in ADC at an earlier stage than subsequent conventional radiological response indicators.

Keywords: *Magnetic resonance imaging; diffusion-weighted; cancer.*

Introduction

The excellent soft tissue contrast of magnetic resonance imaging (MRI) has made it an invaluable technique in oncological assessment. A variety of pulse sequences providing a range of contrast allows detailed evaluation of the size and spread of disease and, to some extent, the heterogeneity within a tumour or its metastases—i.e. the presence of cysts or necrosis or the existence of a vascularised rim. The majority of clinical MR measures the rate at which signal from hydrogen nuclei (protons) in a static magnetic field decays following perturbation by a sequence of rf pulses. This decay is described by the protons' T1 and T2 relaxation rate. Mobile protons, such as those present in a small water molecule, take a relatively long time for their signal to decay in the detector plane and, as a result, the long T2 values produce a large signal on T2-weighted imaging. Protons attached to larger, less mobile fatty molecules have smaller T2 values, that is, their signal decays quickly and results in a lower signal intensity on a T2-weighted image. Pathological processes within tissue such as oedema, necrosis or fibrosis change the water content and vascularity of tissue, and haemorrhage affects local magnetic fields, leading to susceptibility effects. Thus, the presence of a tumour causes changes in the tissue that may alter its T1 or T2 relaxation rates, and be manifest as observable changes on conventional T1- and T2-weighted images. However, changes in T1 and T2 relaxation are often insufficient to detect or characterize the lesion.

Another mechanism for developing image contrast is through 'apparent diffusivity' (the displacement of tissue water due to random, thermally driven motion over distances of ~1–20 μm). The visualization of changes in the diffusion properties of tissue water with MR imaging

has become a useful, multifaceted tool to characterize tissue structure and to identify and differentiate disease processes[1–6]. The degree of motion measured by DW-MRI relates to the mean path length '*L*' travelled by protons in the body within a specific observation time period (its 'diffusion time') as a result of thermally driven, random motion (Fig. 1).

Highly cellular region
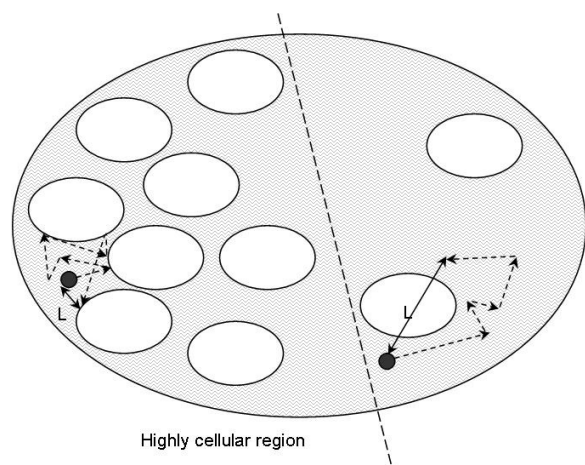
Figure 1   **A representation of a tumour or tissue displaying heterogeneous cellularity. The mean path length '*L*' travelled by protons in the extracellular fluid within a specific observation time is much greater in regions of low cellularity where random motion is not impeded by the presence of cellular membranes.**

Technique

Imaging sequences

The MR signal is made dependent on motion by the inclusion of two additional magnetic field gradients within the pulse sequence. The first gradient pulse alters the phase shift of each proton by an amount dependent on the water molecule's spatial location relative to the gradient. The second gradient pulse (equal and opposite in effect to the first) will reverse this phase shift if the water molecule does not move between the application of the first and second gradient pulses. If there is movement of the water molecule between application of the first and second gradient pulses, then complete rephasing cannot happen, causing signal loss from this spatial location. The amount of signal loss is directly proportional to the degree of water motion, which in turn is dependent on the protons' mean diffusional path length '*L*' (Fig. 2). Figure 2 also demonstrates that signal loss is proportional to the motion component in the same direction as the diffusion gradient. No signal loss would occur if the motion was perpendicular to the gradient direction. DW-MRI is thus sensitive not only to the extent to which protons are free to diffuse but also to their preferential diffusion direction. Both magnitude and direction of diffusion are influenced by the architecture of the tissue under investigation.

Technical limitations

DW-MRI can be adversely affected by artifact from motion other than diffusion. As molecular displacement of the order of micrometres is being observed on diffusion-weighted images, it is no surprise that any motion, even vascular pulsation, interferes with these measurements. Motion present within the body, e.g. voluntary, respiratory, even arteriole level perfusion is capable of producing displacement much greater than that to which DW-MRI has been sensitized. The need to develop 'snap-shot' imaging techniques, to account for bulk motion, has been achieved largely via the implementation of echo-planar imaging (EPI). Single-shot EPI can acquire a complete image within a second, single-shot, or in multiple shots employing navigator MR signals for each shot to correct for bulk motion. While single-shot methods are robust to motion, their elevated sensitivity to magnetic field inhomogeneities leads to image distortion and artifacts in areas exhibiting large variations in magnetic susceptibility, e.g. air–tissue interfaces, or chemical-shift effect, e.g. fat–water interfaces. Owing to the effects of chemical shift, single-shot EPI is performed with fat suppression as standard, the quality of the fat suppression being of great importance in extracranial applications. Spatial resolution tends to be sacrificed to obtain high imaging speeds and signal averaging is likely to be necessary to increase signal-to-noise ratio (SNR), especially when using larger values of diffusion sensitive gradients. A train of single-shot EPI images acquired with a long TR are T2- or T2*-weighted, their effective TE being the time at which the central lines of k-space are filled. Strong frequency encoding gradients enable images to be acquired with a shorter effective TE and consequently better SNR. Multi-shot methods can provide better spatial resolution with fewer image distortion artifacts and higher SNR, but are not as robust to the effects of motion and require acquisition times of 10 min or more.

Image analysis

A DW-MRI sequence's sensitivity to diffusion (characterised by its b-value) can be adjusted by altering the combination of gradient pulse amplitude, the time for which the gradients are applied and the time that elapses between their application (sometimes termed 'diffusion time'). The higher the b-value, the more sensitive an image is to the effects of diffusion.

Even if stringent measures have been taken to avoid the effects of gross motion and flow, a diffusion-weighted image is still affected by MR properties other than that of diffusion, e.g. T2 weighting. To remove all effects other than that of diffusion, the apparent diffusion coefficient
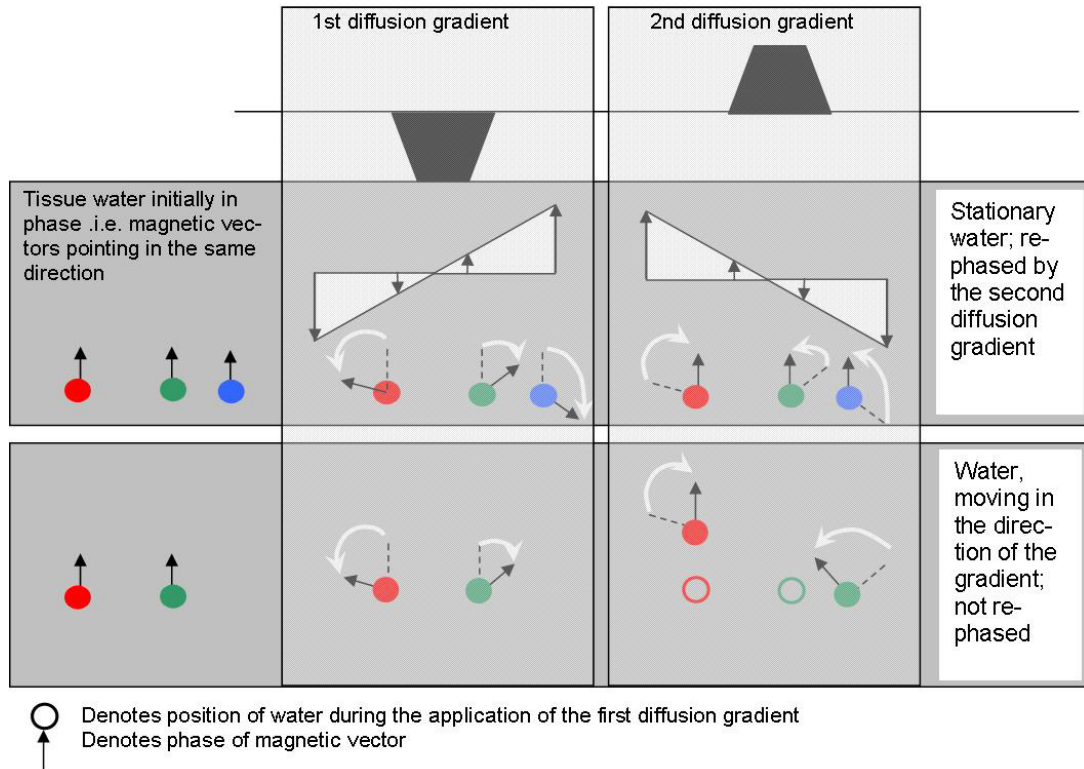
Figure 2   **Signal change during application of diffusion gradients. Water that remains in the same location relative to diffusion gradient experiences firstly the dephasing effects of the first gradient followed by equal and opposite rephasing via the second diffusion gradient: it is not dephased as a result of the diffusion gradients (top row). Water that moves in the direction of the diffusion gradients between their application will experience either too much or too little phase reversal, because it moves to a position where it experiences a different field strength in the second diffusion pulse than it did in the first (lower row, green). The resulting 'dephasing' causes a drop in signal in the diffusion-weighted image. Note that water moving perpendicularly to the diffusion gradient experiences an equal and opposite gradient field strength and is rephased (lower row, red).**

(ADC) map is used. ADC is measured by acquiring the MR signal at least twice, typically with (S_b) and without (S_0) diffusion weighting. Equation 1 describes how two diffusion-weighted images, identical in every way other than their diffusion weighting, can be combined to create an ADC map free of all contrast influences other than the displacement of water during the application of the diffusion gradients.

$$\text{ADC} = \frac{1}{b} \ln \left(\frac{S_0}{S_b} \right). \qquad (1)$$

An ADC map created in this way by combining two images, with and without diffusion weighting or using two b-values, the lower of which is not large enough to remove the effects of perfusion, contains information about perfusion as well as diffusion components. To differentiate between perfusion and diffusion multiple b-values are needed. Figure 3 demonstrates the difference between a diffusion-weighted image and an ADC map. In the diffusion-weighted image protons within a brain tumour are able to diffuse more freely than in surrounding white matter and are associated with a loss of signal.

In the resulting ADC map, the corresponding area of high diffusion is represented as a bright area; a high ADC value. It is therefore crucially important to identify whether a diffusion-weighted image or an ADC map is being presented.

Signal loss in DW-MRI is proportional to the component of molecular displacement in the same direction as that of the diffusion gradient[7]. In some areas of the body, such as in the brain, tissue architecture such as fibre tracts makes it much easier for tissue water to diffuse in a specific direction, e.g. water diffuses preferentially along rather than perpendicular to myelinated axons. This property is exploited in MR tractography where diffusion tensor imaging (DTI) can create a tensor for each image voxel which describes diffusion in multiple directions[8]. At least six independent diffusion-encoding directions are required for such a technique. Alternatively, for some applications, it may be desirable to 'average out' the effects of preferential directions of diffusion. Most clinical machines now offer the capability to create ADC maps by averaging three diffusion-weighted images which have encoded diffusion
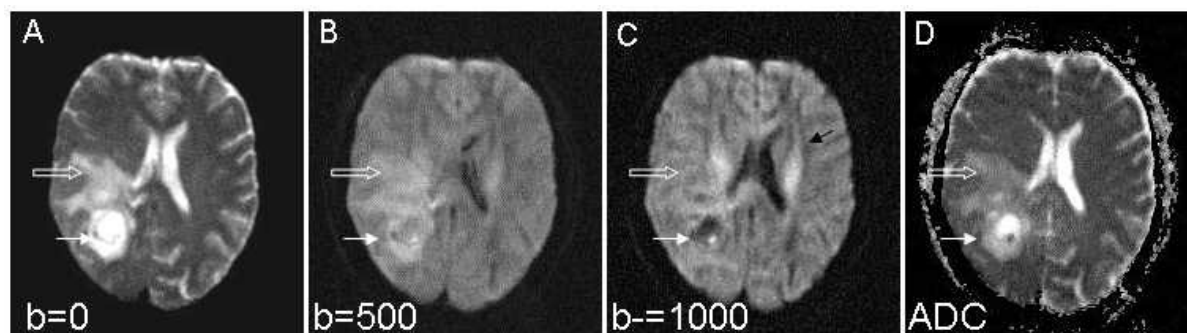
Figure 3   **Primary brain tumour. Transverse DW-MRI (EPI 4184/91 ms [TR/TE]) through the brain at the mid-ventricular level at b-values of 0 (A), 500 (B) and 1000 s/mm^2 (C) sensitized in the antero-posterior direction and isotropic ADC map (D). A mass lesion in the right parieto-occipital region is seen in (A) (arrow) with surrounding high signal intensity from peritumoural oedema in the white matter (open arrow). In (B) there is a reduction of signal from within the tumour which becomes more marked as diffusion weighting increases ((C), arrow). This reflects breakdown of brain tissue structure and increased diffusion. On the ADC map this region of tumour with high diffusivity is bright. In the surrounding oedematous tissue water diffuses less freely because of intact tissue architecture (open arrow). Note also the high diffusivity in the ventricular CSF and in the white matter tracts running antero-posteriorly in the direction of diffusion sensitization ((C), black arrow). The anisotropic diffusion within the white matter tracts is not represented in the 'trace' ADC image (D).**

in the slice, frequency (read) and phase-encode directions respectively. Such techniques are termed 'isotropic' and the associated averaged ADC maps sometimes termed 'trace' or 'isotropic'.

Pathological correlates

The majority of DW-MRI performed clinically to date has focused on the measurement of extracellular water diffusion. In tissues, the random paths extracellular water molecules may otherwise take are hindered by structural interfaces. In a highly cellular tissue, extracellular water would not be able to diffuse far during the MR observation period without being blocked by cell membranes; this would lead to a short diffusional path and a reduced ADC (Fig. 3). Conversely, in cystic or necrotic portions of tumours with fewer structural barriers present, the diffusional path-length would be associated with a high ADC value. ADC maps, derived from diffusion-weighted imaging, can therefore provide a non-invasive measure of cellularity[9]. In terms of oncological imaging this has obvious potential for diagnosis, treatment planning and monitoring.

Animal systems have been used to separate extracellular and intracellular components of tissue diffusion. Diffusion of water in the extracellular microenvironment is approximately two-fold slower than that of free water while diffusion within the intracellular compartment is about one order of magnitude slower than that of free water. By using a broad range of diffusion times and gradient strengths it was possible to distinguish water diffusion in extracellular and intracellular compartments in hormonal-dependent MCF7 breast tumours implanted orthotopically in immunodeficient mice, and evaluate the effect of restricted diffusion and water exchange on the water diffusion in these compartments[10]. Pixel-by-pixel analysis yielded parametric maps of the estimated volume fraction and apparent diffusion coefficient of each compartment. Mapping of the water fraction in each compartment can make DW-MRI more specific to changes during tumour progression and response. Hormonal manipulation with the antiestrogenic drug tamoxifen methiodide showed that in parallel with the growth arrest by this drug, the volume fraction of the slowly diffusing water increased, suggesting a tamoxifen-induced cell swelling.

Novel diagnostic applications

Le Bihan in 1986[11], and Moseley in 1990[12] conducted ground-breaking animal studies that demonstrated the value of DW-MRI for the early detection of stroke. Since then, DW-MRI has been used in both clinical and research settings for detecting cerebral ischaemia as well as cancer-related pathologies. In cancer imaging, it has been used primarily in characterizing brain tumours although a number of important applications in the body are emerging.

Brain

In the early days of DW-MRI, apparent diffusion coefficient (ADC) maps of brain tumours provided useful information regarding the architecture of the tissue, but were not particularly helpful for the characterization of
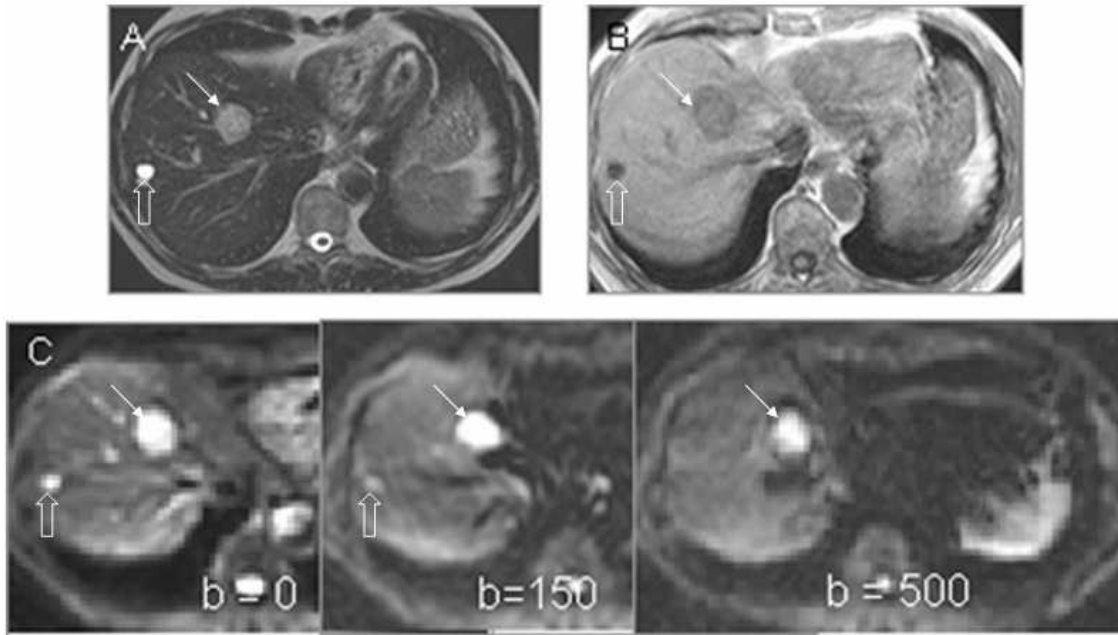
Figure 4 **Liver metastasis from colorectal cancer. Transverse T2W (FSE 2500/80 ms [TR/TE] (A), post-contrast T1W (GRE 200/12/70^0 ms [TR/TE/FA] (B), and diffusion-weighted images (single-shot EPI 1850/56 ms [TR/TE], (C) (b = 0, 150, 500 s/mm^2) through the liver showing a metastatic deposit (arrow) and a cyst (open arrow). The metastasis shows increasingly restricted diffusion at increasing b-values. Signal from the cyst on the other hand decays away as diffusivity is high.**

tumour vs. peritumoural oedema compared to standard contrast-enhanced imaging. This was related to the choice of b-values: routine diffusion imaging of the brain generally involved the use of b-factors within the range of 0–1000 s/mm^2. ADC maps were then generated, based on the assumption that the relationship between the MR signal and b-factor was monoexponential. It has been shown by using multiple b-factors of up to 6000 s/mm^2 that the signal decay is better described with a bi-exponential curve[13], that is, more that one distinct value of ADC is present. As signal losses due to perfusion effects are only observed with b-factors of less than 300 s/mm^2, exclusion of low b-values (and thus perfusion effects) and use of a bi-exponential fit for larger b-values shows greater distinction between tumour, peritumoural oedema and normal white matter. The fast diffusion component of both tumour tissue and peritumoural oedema is increased by almost 50% compared with the value in white matter, while the slow component increases significantly in tumour tissue compared to peritumoural oedema. Variable changes also occur within tumour tissue itself, which reflects the fact that tumours do not represent a single tissue type; for example, cystic regions are easily distinguished by their mono-exponential diffusion and high ADC (Fig. 3). Thus in DW-MRI employing low b-values peritumoural oedema and tumour tissue are both brighter than white matter; at increased diffusion weighting (500–1000 s/mm^2) the contrast between the different tissues is minimal; and at very high diffusion weighting tumour tissue is brighter than white matter and peritumoural oedema since tumour has a higher signal amplitude arising from its slow-diffusing component[14]. Increasingly the clinical utility of these images to provide a surrogate marker for treatment response in patient studies is becoming apparent[5,15]. Diffusion tensor imaging adds further information about the directional dependence of molecular diffusion and may also help in demarcating tumour margins and in defining the relationship of the tumour to fibre tracts prior to surgical excision.

Head and neck

DW-MRI has also been applied in head and neck tumours. One large study by Wang *et al.* in 2001[16] that included 81 evaluable lesions (carcinomas, lymphomas, benign salivary gland adenomas and benign cysts) showed that there was a significant difference in the ADCs of the four groups of lesions. Surprisingly only 16% of lesions were not evaluable because of distortion artifacts. These lesions were predominantly around airspaces—in the paranasal sinuses or larynx. DW-MRI thus may have some role in lesion characterization in the head and neck, although the anatomical site of the lesion is the overriding factor in determining diagnosis.
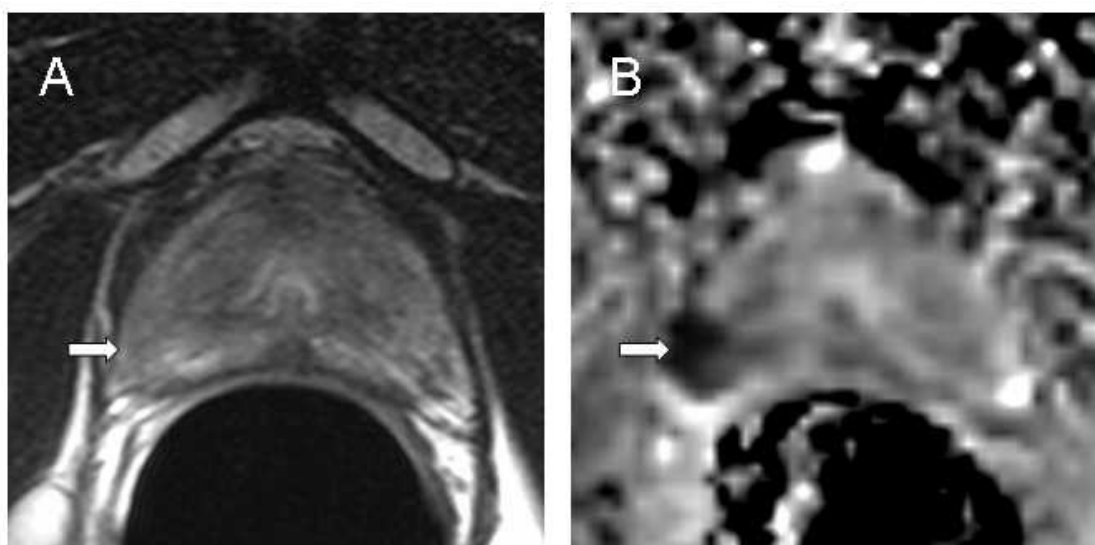
Figure 5 **Primary prostate cancer. Transverse T2W image (FSE 2096/90 ms [TR/effective TE] (A) and an isotropic ADC map (B) at the same level through the prostate apex calculated from images (b = 0, 300, 500, 800 s/mm^2) with diffusion-weighted gradients sensitised in three planes. The tumour which is poorly seen as an ill-defined low-signal intensity area on T2W (arrow) is clearly demarcated as an area of restricted diffusion (arrow) on the ADC map.**

Breast

DW-MRI has been applied to diagnose breast cancer and identify cancer extension[17,18]. Isotropic DW-MRI performed with echo-planar sequences (b-values 0, 750 and 1000 s/mm^2) showed that the mean ADC value of breast cancer was $1.12 +/- 0.24 \times 10^{-3}$ mm^2/s, which was lower than that of normal breast tissue, and that the sensitivity of the ADC value for breast cancer using a threshold of less than 1.6×10^{-3} mm^2/s was 95%. Also, the ADC value for invasive ductal carcinoma was lower than that of noninvasive ductal carcinoma. Seventy-five percent of all cases showed precise distribution of low ADC value as cancer extension. Guo *et al.*[19] also confirmed that DW-MRI may be potentially useful in distinguishing between malignant and benign breast lesions. Further, tumour cellularity has a significant influence on the ADCs obtained in both benign and malignant breast tumours. Limitations of the technique in the breast arise from underestimation of ADC, primarily due to susceptibility artifact from blood products and the limit of spatial resolution.

Liver

In the liver, DW-MRI measurements have been plagued by poor motion compensation. Recently, use of an echo-planar technique with breath-hold has allowed relatively robust mapping of lesions in the right lobe of the liver[20]. Cardiac triggering has proved useful in some cases. In the left lobe, cardiac and abdominal wall motion reduce the sensitivity of the technique. However, data from phantom studies suggest that a free-breathing technique may be possible[21]. In multiple studies quantitative measures of ADC in abdominal organs and liver lesions have been achieved, but discrepancies in the mean ADC values remain and are associated with the choice of b-values used. Low b-values of under 55 s/mm^2 lead to overestimation of ADC due to the contribution of perfusion to the diffusion measurement, while use of large b-values over 1200 s/mm^2 underestimate the ADC[22] due to low SNR. A range of b-values from zero up to a maximum of 1000 s/mm^2 with a more common maximum value of 500 s/mm^2 produces better quality diffusion-weighted images and ADCs that are within the same range. A significant difference in ADC value between benign and malignant liver lesions allows them to be differentiated (Fig. 4), but comparison between studies is still difficult owing to variation in the data. However, ADC accuracy may be improved by reducing artifacts through use of techniques such as parallel imaging. Multiple diffusion gradient directions are not necessarily useful as the liver appears isotropic with no demonstrable difference in reported ADC values related to the direction of the diffusion gradient[23]. Early data are also showing that ADC may predict the response of hepatic metastases to treatment[24], as low pre-treatment ADCs correspond to a subsequent good therapeutic response.

Prostate

There are a few recent reports of the utility of DW-MRI in prostate cancer, where its role appears promising but
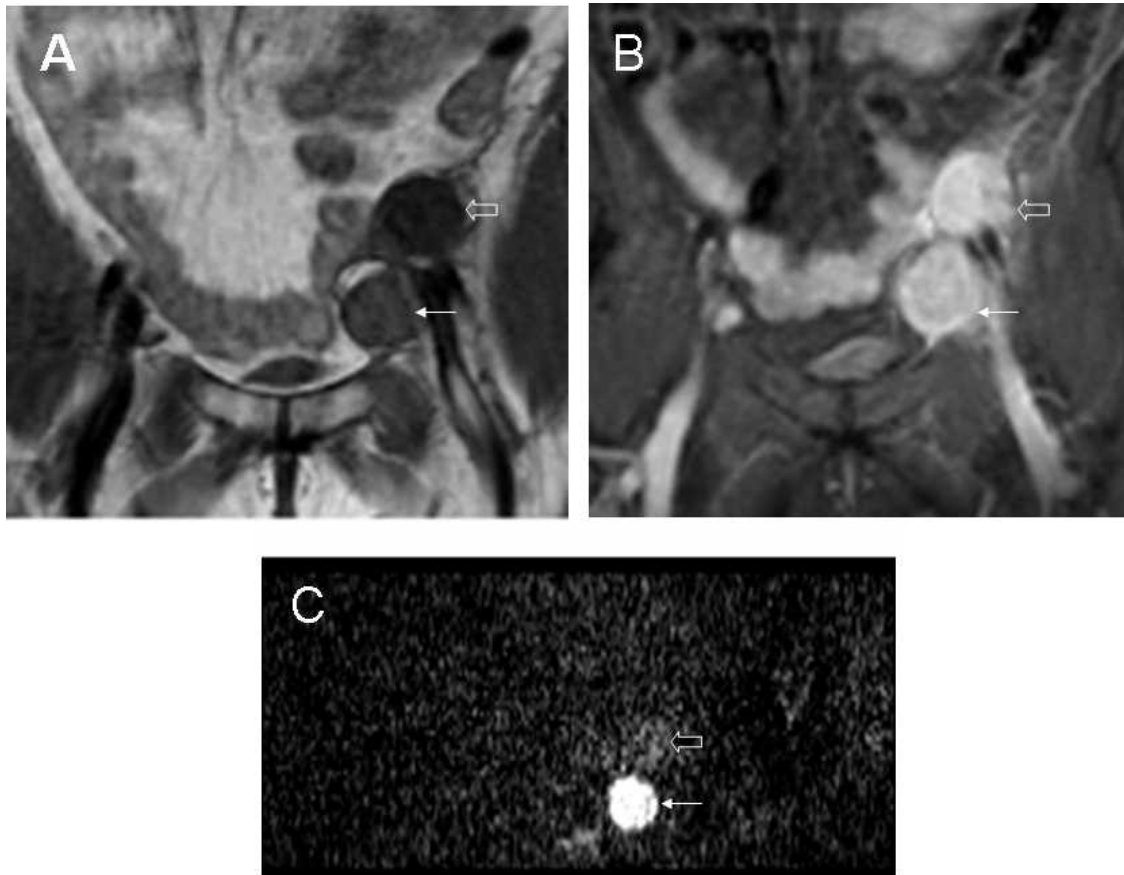
Figure 6   **Recurrent ovarian cancer. Coronal T1W (FSE 600/14 ms [TR/TE] (A), STIR (IR 1833/15/165 ms [TR/TE/TI] (B) images and maximum intensity projection of a whole body diffusion-weighted image ((C), b = 0, 1000 s/mm^2) showing left pelvic side-wall lymphadenopathy. Although the nodes are well defined in (A) and (B), the differentiation between cystic (open arrow) and solid (small arrow) component of tumour is clearly apparent on the diffusion-weighted image.**

has not been established. The extensive branching ductal structure of the normal prostate compared with the highly restricted intracellular and interstitial spaces encountered in prostate cancers produces a substantial differential in ADC and, thus, the potential for high image contrast (Fig. 5). Also, the ADC values of malignant prostate nodules appear significantly lower than in non-malignant prostate tissue[25]. This has particular implications for identifying the 30% of cancers that arise within the central gland. Improved discrimination of malignant tissue in both the peripheral and central zones of the prostate would improve local staging performance, increase accuracy in performing biopsy, focusing of irradiation for intensity-modulated radiotherapy, follow-up of therapy response, and earlier detection of tumour recurrence. For DW-MRI of the prostate, single-shot echo-planar sequences are favoured over turbo spin-echo sequences because of the need to freeze bulk motion. However, the susceptibility-induced distortion to which single-shot EPI is prone can be problematic in prostate imaging where air in the rectum or within the balloon of the endorectal coil causes significant local

magnetic field inhomogeneity and susceptibility artifact. In future, use of DW-MRI as an adjunct to T2-weighted sequences would complement techniques such as MR spectroscopy and dynamic contrast-enhanced imaging which are increasingly used in tumour detection. It may also be valuable for characterization of highly cellular regions of tumours versus acellular regions, as well as for detecting treatment response, manifested as a change in cellularity within the tumour over time.

Whole body studies

Until recently, DW-MRI for whole body malignancy screening has been significantly limited because of relatively thick slices required (to achieve coverage during a breath-hold) and unreliable fat suppression. Takahara *et al.*[26] have developed a multiple thin slice whole body DW-MRI using: (a) a free-breathing approach that affords multiple slice excitations and signal averaging over an extended period of time; and (b) a short TI inversion recovery (STIR)-EPI sequence that allows potent fat suppression, which improves the quality

of the 3D reconstructed images in whole body imaging. The sequence provides good background body signal suppression including vessel, muscle and fat signal by the heavy diffusion weighting and/or the STIR pulse. The longer scan time affords more slices with multiple signal averaging, higher SNR, and potent fat suppression, enabling quality MIP reconstruction. Also, the free breathing averages out unwanted signal. The STIR pulse is useful for the detection of lesions because most of the pathologic lesions have increased free water, and thus prolonged T1 and T2 values, resulting in a bright signal on STIR. STIR also may be useful in suppressing the intestinal signal that has a short T1 value. However, SNR is lower in STIR than in spin-echo, which makes it time-consuming, with an average acquisition time of 10 min for a 60-slice coverage. Images are displayed with an inverted grey-white scale familiar to clinicians, as they resemble those seen in scintigraphy or in PET (Fig. 6). A disadvantage is that only one b-value of 1000 s/mm^2 is used, and reliable ADC values cannot be obtained. Adding b-values is feasible, but prolongs acquisition time.

Prediction and early monitoring of treatment response

DWI-MRI is being widely used to assess treatment response [27–29]. Mardor *et al.* in 2004 [30] demonstrated that pre-treatment ADC values of primary and metastatic malignant brain lesions could predict response to radiotherapy treatment, i.e. tumours with higher ADCs responded less favourably. The regions of interest used in this work were defined over the entire apparent tumour on the contrast-enhanced T1-weighted image and included necrotic or cystic portions of the tumour in the ADC analysis. In patients with locally advanced rectal cancer, low mean pre-treatment tumour ADC predicted for a larger percentage size change of tumours after chemotherapy [31]. Quantitative DW-MRI also has been shown to have potential to predict response of colorectal hepatic metastases to chemotherapy: a high pre-treatment ADC predicts for a poor response [32]. The results of each of these studies are consistent with the hypothesis that a high ADC may be indicative of tumour necrosis and consequently greater resistance to treatment. Animal and clinical studies have reported that an increase in ADC values early after treatment initiation is associated with a subsequent reduction in tumour volume. Similarly, in clinical studies Galons *et al.* [6] demonstrated that a clear, substantial, and early increase in the ADC after successful therapy in drug sensitive breast tumours treated with paclitaxel was potentially of great value in identifying response within a much shorter time-scale than the associated changes in gross tumour volume. Theilman *et al.* showed that in 60 measurable liver metastases from breast cancer monitored by diffusion MRI after initiation of new courses of chemotherapy, DW-MRI predicted response by 4 or 11 days after commencement of therapy, particularly in tumour lesions that were less than 8 cm^3 in volume at presentation [24]. These observations are thought to be associated with an initial decrease in tumour cellularity in response to cell kill (and subsequent increase in extracellular space) reflected in an increase in tumour ADC value.

Conclusion

Diffusion-weighted imaging offers huge potential in oncology. It is relatively easy to implement, and echo-planar single- and multi-shot imaging incur very little time penalty as part of a standard MR examination. Image distortion and motion artifacts remain limitations, but its ability for quantification of data and ease of therapy monitoring ensure its future as an invaluable diagnostic tool.

Acknowledgements

References

[1] Mori S, Barker PB. Diffusion magnetic resonance imaging: its principle and applications. Anat Rec 1999; 257: 102–9.

[2] Gibbs P, Tozer DJ, Liney GP, Turnbull LW. Comparison of quantitative T2 mapping and diffusion-weighted imaging in the normal and pathologic prostate. Magn Reson Med 2001; 46: 1054–8.

[3] Maier CF, Paran Y, Bendel P, Rutt BK, Degani H. Quantitative diffusion imaging in implanted human breast tumors. Magn Reson Med 1997; 37: 576–81.

[4] Gupta RK, Cloughesy TF, Sinha U, Garakian J, Lazareff J, Rubino G *et al*. Relationships between choline magnetic resonance spectroscopy, apparent diffusion coefficient and quantitative histopathology in human glioma. J Neurooncol 2000; 50: 215–26.

[5] Chenevert TL, Stegman LD, Taylor JM, Robertson PL, Green-berg HS, Rehemtulla A *et al*. Diffusion magnetic resonance imaging: an early surrogate marker of therapeutic efficacy in brain tumors. J Natl Cancer Inst 2000; 92: 2029–36.

[6] Galons JP, Altbach MI, Paine-Murrieta GD, Taylor CW, Gillies RJ. Early increases in breast tumor xenograft water mobility in response to paclitaxel therapy detected by non-invasive diffusion magnetic resonance imaging. Neoplasia 1999; 1: 113–17.

[7] Rowley HA, Grant PE, Roberts TP. Diffusion MR imaging: theory and applications. Neuroimaging Clin N Am 1999; 9: 343–61.

[8] Le Bihan D, Mangin JF, Poupon C, Clark CA, Pappata S, Molko N *et al*. Diffusion tensor imaging: concepts and applications. J Magn Reson Imaging 2001; 13: 534–46.

[9] Herneth AM, Guccione S, Bednarski M. Apparent diffusion coefficient: a quantitative parameter for in vivo tumor character-ization. Eur J Radiol 2003; 45: 208–13.

[10] Paran Y, Bendel P, Margalit R, Degani H. Water diffusion in the different microenvironments of breast cancer. NMR Biomed 2004; 17: 170–80.

[11] Le Bihan D, Breton E, Lallemand D, Grenier P, Cabanis E, Laval-Jeantet M. MR imaging of intravoxel incoherent motions: application to diffusion and perfusion in neurologic disorders. Radiology 1986; 161: 401–7.

[12] Moseley ME, Kucharczyk J, Mintorovitch J, Cohen Y, Kurhanewicz J, Derugin N *et al*. Diffusion-weighted MR imaging of acute stroke: correlation with T2-weighted and magnetic susceptibility-enhanced MR imaging in cats. AJNR Am J Neuroradiol 1990; 11: 423–9.

[13] Mulkern RV, Gudbjartsson H, Westin CF, Zengingonul HP, Gartner W, Guttmann CR *et al*. Multi-component apparent diffusion coefficients in human brain. NMR Biomed 1999; 12: 51–62.

[14] Maier SE, Bogner P, Bajzik G, Mamata H, Mamata Y, Repa I *et al*. Normal brain and brain tumor: multicomponent apparent diffusion coefficient line scan imaging. Radiology 2001; 219: 842–9.

[15] Chenevert TL, Meyer CR, Moffat BA, Rehemtulla A, Mukherji SK, Gebarski SS *et al*. Diffusion MRI: a New strategy for assessment of cancer therapeutic efficacy. Mol Imaging 2002; 1: 336–43.

[16] Wang J, Takashima S, Takayama F, Kawakami S, Saito A, Matsushita T *et al*. Head and neck lesions: characterization with diffusion-weighted echo-planar MR imaging. Radiology 2001; 220: 621–30.

[17] Woodhams R, Matsunaga K, Iwabuchi K, Kan S, Hata H, Kuranami M *et al*. Diffusion-weighted imaging of malignant breast tumors: the usefulness of apparent diffusion coefficient (ADC) value and ADC map for the detection of malignant breast tumors and evaluation of cancer extension. J Comput Assist Tomogr 2005; 29: 644–9.

[18] Kuroki Y, Nasu K, Kuroki S, Murakami K, Hayashi T, Sekiguchi R *et al*. Diffusion-weighted imaging of breast cancer with the sensitivity encoding technique: analysis of the apparent diffusion coefficient value. Magn Reson Med Sci 2004; 3: 79–85.

[19] Guo Y, Cai YQ, Cai ZL, Gao YG, An NY, Ma L *et al*. Differentiation of clinically benign and malignant breast lesions using diffusion-weighted imaging. J Magn Reson Imaging 2002; 16: 172–8.

[20] Koh DM, Scurr E, Collins DJ, Pirgon A, Kanber B, Karanjia N *et al*. Colorectal hepatic metastases: quantitative measurements using single-shot echo-planar diffusion-weighted MR imaging. Eur Radiol 2006 May 12 [Epub ahead of print].

[21] Muro I, Takahara T, Horie T, Honda M, Kamiya A, Okumura Y *et al*. [Influence of respiratory motion in body diffusion weighted imaging under free breathing (examination of a moving phantom)]. Nippon Hoshasen Gijutsu Gakkai Zasshi 2005; 61: 1551–8.

[22] Namimoto T, Yamashita Y, Sumi S, Tang Y, Takahashi M. Focal liver masses: characterization with diffusion-weighted echo-planar MR imaging. Radiology 1997; 204: 739–44.

[23] Taouli B, Vilgrain V, Dumont E, Daire JL, Fan B, Menu Y. Evaluation of liver diffusion isotropy and characterization of focal hepatic lesions with two single-shot echo-planar MR imaging sequences: prospective study in 66 patients. Radiology 2003; 226: 71–8.

[24] Theilmann RJ, Borders R, Trouard TP, Xia G, Outwater E, Ranger-Moore J *et al*. Changes in water mobility measured by diffusion MRI predict response of metastatic breast cancer to chemotherapy. Neoplasia 2004; 6: 831–7.

[25] Hosseinzadeh K, Schwarz SD. Endorectal diffusion-weighted imaging in prostate cancer to differentiate malignant and benign peripheral zone tissue. J Magn Reson Imaging 2004; 20: 654–61.

[26] Takahara T, Imai Y, Yamashita T, Yasuda S, Nasu S, Van Cauteren M. Diffusion weighted whole body imaging with background body signal suppression (DWIBS): technical improvement using free breathing, STIR and high resolution 3D display. Radiat Med 2004; 22: 275–82.

[27] Provenzale JM, Mukundan S, Barboriak DP. Diffusion-weighted and perfusion MR imaging for brain tumor characterization and assessment of treatment response. Radiology 2006; 239: 632–49.

[28] Manton DJ, Chaturvedi A, Hubbard A, Lind MJ, Lowry M, Maraveyas A *et al*. Neoadjuvant chemotherapy in breast cancer: early response prediction with quantitative MR imaging and spectroscopy. Br J Cancer 2006; 94: 427–35.

[29] Thoeny HC, De Keyzer F, Chen F, Ni Y, Landuyt W, Verbeken EK *et al*. Diffusion-weighted MR imaging in monitoring the effect of a vascular targeting agent on rhabdomyosarcoma in rats. Radiology 2005; 234: 756–64.

[30] Mardor Y, Roth Y, Ochershvilli A, Spiegelmann R, Tichler T, Daniels D *et al*. Pretreatment prediction of brain tumors' response to radiation therapy using high b-value diffusion-weighted MRI. Neoplasia 2004; 6: 136–42.

[31] Dzik-Jurasz A, Domenig C, George M, Wolber J, Padhani A, Brown G *et al*. Diffusion MRI for prediction of response of rectal cancer to chemoradiation. Lancet 2002; 360 (9329): 307–8.

[32] Scurr E, Collins DJ, Kanber B, Riddell A, Brown G, deSouza NM *et al*. Detection of colorectal liver metastases by diffusion-weighted imaging. Proc Int Soc Mag Reson Med 2006; 14: 401 [Abstract].